Born effective charges and infrared response of LiBC

Kwan-Woo Lee and W. E. Pickett
Department of Physics, University of California, Davis, California 95616, USA
(Received 27 February 2003; published 13 August 2003)

Calculations of the zone-center optical-mode frequencies (including LO-TO splitting), Born effective charges $Z^*_{\alpha\alpha}$ for each atom, dielectric constants ϵ_0 and ϵ_∞, and the dielectric response in the infrared, using density functional linear response theory, are reported. Calculated Raman modes are in excellent agreement with experimental values (170 cm^{-1} and 1170 cm^{-1}), while it will require better experimental data to clarify the infrared-active mode frequencies. The Born effective charges $Z^*_{\alpha\alpha}$ (i) have surprisingly different values for B and C and (ii) show considerable anisotropy. Relationships between the effective charges and LO-TO splitting are discussed, and the predicted reflectivity in the range 0–1400 cm^{-1} is presented. These results hold possible implications for Li removal in LiBC and C substition for B in MgB_2.

DOI: 10.1103/PhysRevB.68.085308 PACS number(s): 77.22.−d, 78.30.−j, 63.20.−e

I. INTRODUCTION

The discovery of superconductivity near 40 K in MgB_2 (Ref. 1) and the rapid development in the understanding of the microscopic mechanism (a specific type of electron-phonon coupling) has spurred extensive work on its properties and the discovery of closely related materials. Interest in LiBC and its Li-deficient derivatives has been spurred by calculational evidence[2] that the electron-phonon coupling will be stronger, and consequently the superconducting transition temperature is expected to be higher, than MgB_2. LiBC is isostructural to, and isovalent with, MgB_2 to the extent possible in a ternary compound, as we discuss more below.

LiBC was first synthesized by Wörle *et al.*,[3] who provided the crystal structure and also reported hole doping by removal of Li, which changed it from reddish in color to black and increased the conductivity. Recently there has been renewed interest in synthesizing this compound and studying its properties. Bharathi *et al.* studied synthesis for varying starting concentrations of Li,[4] but did not report any samples becoming metallic. Hlinka and co-workers presented Raman scattering measurements on few-micron-size crystallites,[5] finding modes at 170 cm^{-1} and 1176 cm^{-1}, which were recently confirmed by Renker *et al.* (171 and 1167 cm^{-1}).[6] Souptel *et al.* focused on the synthesis of samples for varying flux concentrations and, like Bharathi *et al.*, found conductivities characteristic of lightly doped semiconductors.[7] Optical studies on LiBC were begun by Pronin *et al.* using an infrared microscope on small crystals,[8] providing infrared (IR) reflectivity in the 400–1900 cm^{-1} range and measurements of the dielectric behavior at lower frequencies. We will return below to a discussion of the implications of the Raman and IR data for the vibrational properties of LiBC.

As for possible doping (deintercalation of Li), all of these reports are probably consistent with very low doping, too low to drive the material conducting (in spite of the broad bands that promote doped-hole conduction). The susceptibility data indicate small concentrations of local moments, typical of semiconductors with point defects. Zhao, Klavins, and Liu, in their efforts at Li deintercalation, observed evaporation of Li upon vacuum annealing, with no sign of superconductivity in the annealed samples.[9] The amount of Li remaining in the sample has not yet been characterized, however (x rays are not sensitive enough), so definitive results remain to be obtained.

The purpose of this paper is to obtain in more detail the character of the intrinsic (insulating) phase of LiBC. Phonon frequencies calculated by linear response techniques using the full-potential linear muffin-tin orbital (FP-LMTO) method were calculated by An *et al.*[10] In this paper we use related extended methods to calculate not only the phonon frequencies (again, with different codes) but the dynamic effective charge tensor Z^*_α, the longitudinal-transverse (LO-TO) mode splittings, oscillator strengths of the IR active phonons, and related dynamic dielectric behavior. Since Li is known, from calculations, to be ionic in this compound, one could anticipate $Z^*_{Li} \approx +1$, and because B and C lie side by side in the periodic table, $Z^*_B \approx Z^*_C$ and of course $Z^*_B + Z^*_C = -Z^*_{Li}$ from the acoustic sum rule. We find much more interesting behavior, however; Z^*_B and Z^*_C are of opposite sign and large — they behave like strongly charged cations and anions, respectively. We analyze this behavior and also comment on the possible relevance this behavior has for the difficulty in deintercalating Li from LiBC and also for C doping in $MgB_{2-x}C_x$.

II. CALCULATIONAL METHODS

The calculations were carried using the ABINIT code with Troullier-Martins pseudopotentials,[11,12] Teter parametrization[13] of the Ceperley-Alder exchange-correlation potential, and 216 **k** points in the irreducible wedge of the Brillouin zone. The kinetic energy cutoff for the plane waves was 60 hartrees. The *f* sum rule (relative to unity) (Ref. 14) was satisfied to 0.05%, which is one measure that the basis set is effectively complete. The experiment lattice constants ($a = 2.752$ Å, $c = 7.058$ Å) (Ref. 3) of LiBC (space group $P6_3/mmc$, No. 194) were used. The calculation of effective charges follows the formalism of Gonze and Lee[15] as implemented in the ABINIT code.

The crystal structure of LiBC, pictured in Fig. 1, is a direct generalization of that of MgB_2. The B and C atoms

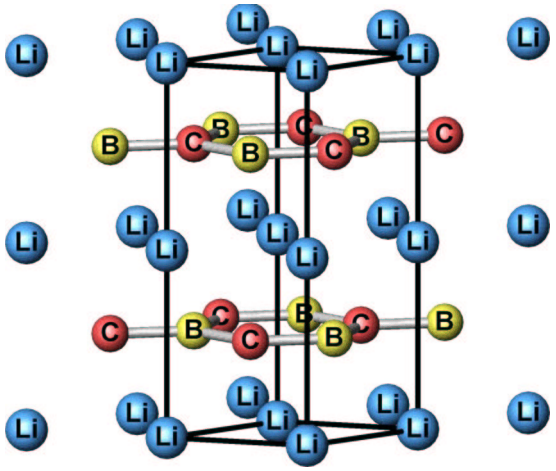

FIG. 1. Crystal structure of LiBC, showing the alternating B-C arrangement in the graphene layers. B and C atoms also alternate along the $\hat{c}$ axis, resulting in two layers and two formula units per primitive cell. The Li ions reside in the interstitial positions between B-C hexagonal rings above and below.

form a flat graphene sheet, with B and C atoms alternating around each hexagonal unit. The stacking of B-C layers is alternating, such that each B has C neighbors along the $\hat{c}$ direction and similarly for C. This stacking, which doubles the unit-cell volume over that of MgB_2, indicates that B-C bonding along $\hat{c}$ (to the extent that it occurs) is preferable to B-B and C-C bonding. Possibly this stacking results in a favorable Madelung energy, although real static charges associated with B and C separately are almost impossible to define or calculate. The Li ions lie in the interstitial site (center of inversion) between the centers of the hexagonal units above and below, coordinated at equal distances with six B atoms and six C atoms.

III. RESULTS

A. Vibrational frequencies

The character of the various zone-center modes in LiBC were presented earlier by An *et al.*[10] For completeness, we repeat them here, with our calculated frequencies (in cm^{-1}), with macroscopic electric field contributions neglected; those corrections and LO-TO splittings are discussed below. Factor group analysis[16] at the Γ point yields 15 optical modes: $2A_{2u}+2B_{1g}+B_{2u}$ with motions along the $\hat{c}$ direction and $2E_{1u}+2E_{2g}+E_{2u}$ with motions in the $a-b$ plane (the latter type are all twofold-degenerate E modes). The $2A_{2u}$ and $2E_{1u}$ are infrared active and the $2E_{2g}$ modes are Raman active:[5,6,8,10]

$\omega=169$: E_{2g}, B-C layers sliding against each other

$\omega=299$: B_{2g}, B-C layers beating against each other along $\hat{c}$

$\omega=292$: E_{2u}, Li layers sliding against each other

$\omega=346$: E_{1u}, Li layers sliding against the B-C layers

$\omega=407$: A_{2u}, Li layers beating against the B-C layers, along $\hat{c}$

TABLE I. Zone-center optical modes of LiBC. The first column ($\mathbf{E}=0$) is for no electric field, the second is for the field lying in the plane ($\mathbf{E}\perp\hat{c}$), and the third is for $\mathbf{E}\|\hat{c}$. The $2A_{2u}$ and $2E_{1u}$ are infrared active and the $2E_{2g}$ modes are Raman active. $\Delta\omega^2=\omega_{LO}^2-\omega_{TO}^2$.

Mode Symmetry	Phonon frequency (cm^{-1}) $\mathbf{E}=0$	$\mathbf{E}\|a-b$	$\mathbf{E}\|\hat{c}$	$\sqrt{\Delta\omega^2}$ (cm^{-1})
E_{2g}	169	169	169	
	169	169	169	
E_{2u}	292	292	292	
	292	292	292	
B_{2g}	299	299	299	
E_{1u}	346	346	346	
	346	**371**	346	135
A_{2u}	407	407	**507**	302
B_{2u}	510	510	510	
A_{2u}	803	803	**828**	200
B_{1g}	829	829	829	
E_{1u}	1143	1143	1143	
	1143	**1235**	1143	469
E_{2g}	1153	1153	1153	
	1153	1153	1153	

$\omega=510$: B_{1u}, Li layers beating against each other along $\hat{c}$

$\omega=803$: A_{2u}, B-C puckering mode, all B atoms move oppositely to all C atoms, Li sites become inequivalent

$\omega=829$: B_{2g}, B-C puckering mode, B moves with C atoms above or below it, Li sites remain equivalent

$\omega=1143$: E_{1u}, B-C bond stretching mode, the two layers are out of phase

$\omega=1153$: E_{2g}, B-C bond stretching mode, layers in phase

Our calculated values are also provided in Table I, where LO-TO splittings, where they arise, are also presented. Compared with the observed Raman-active modes at 170 and 1176 cm^{-1} (Ref. 5) and 171 and 1167 cm^{-1} (Ref. 6), the calculated values 169 and 1153 cm^{-1} are in excellent agreement.

The LO-TO splitting for displacement parallel to the layers occurs for the "layer sliding" mode at 346 cm^{-1} ($\Delta\omega=25$ cm^{-1}) and for the B-C "bond stretching" mode at 1143 cm^{-1} ($\Delta\omega=92$ cm^{-1}). For $\hat{c}$ polarization, the "layer beating" mode is at 407 cm^{-1} ($\Delta\omega=100$ cm^{-1}), and the B-C "puckering" mode at 803 cm^{-1} is split by only $\Delta\omega=25$ cm^{-1}. The large LO-TO splittings of the "layer beating" and "bond stretching" modes suggest they involve large effective charges, as we confirm below.

Data on IR-active modes have been published by Pronin *et al.*[8] who fit reflectivity data with modes at 540, 620, 700 (less clear), and 1180 cm^{-1}. The highest (and strong in the data) mode is close to our calculated value (TO 1143 cm^{-1}, LO 1235 cm^{-1}), but the others are difficult to assign. The data, with three or four positions of structure, apparently in-

TABLE II. The Born effective charges of LiBC. The acoustic sum rule $\Sigma_s Z_s^* = 0$ is fulfilled to within 0.01. $\overline{Z^*} = (1/3)\ \mathrm{Tr}\mathbf{Z}^*$.

	Z^*(Li)	Z^*(B)	Z^*(C)
$\mathbf{Z}_\parallel^*$	0.81	2.37	−3.17
$\mathbf{Z}_\perp^*$	1.46	0.61	−2.07
$\overline{Z^*}$	1.03	1.78	−2.80

clude contributions from $\hat{c}$-axis polarization, $a-b$ plane polarization, and all angles between. Bharathi *et al.* have presented IR absorption spectra[4] with main peaks at ~380, 950, and 1200 cm^{-1}. The lower and upper of these are not far from our calculated values for E_{1g} modes (Table I), but the nearest IR mode to the 950 cm^{-1} peak is our A_{2u} mode at 803–828 cm^{-1}.

B. Effective charges and oscillator strengths

In a noncubic lattice the Born (dynamical) effective charge of an ion becomes a tensor. In hexagonal symmetry such as in LiBC, the tensor is diagonal and reduces to two values $Z_{xx}^* = Z_{yy}^* \equiv Z_\parallel^*$ and $Z_{zz}^* \equiv Z_\perp^*$. These charges, which show considerable anisotropy in LiBC, are given in Table II. The acoustic sum rule $\Sigma_s Z_s^* = 0$ is fulfilled to within 0.01, suggesting well-converged calculations. In spite of the fact that they are neighbors in the periodic table and that both B and C are comfortable forming the graphene structure layer, when they alternate in this graphene layer their effective charges are vastly different: substantial in size but different in sign. Given their similarities, the effective charge sum rule, and that Li is ionized, one might perhaps expect values close to $+1$, 0, and -1 (or possibly $+1$, $-\frac{1}{2}$, and $-\frac{1}{2}$) for Li, B, and C, respectively. They are, on (angular) average, much closer to the values $+1,+2$, and -3, which are not so far from the bizarre ionic configuration (the only one with closed shells) of $+1,+3$, and -4 for Li, B, and C, respectively, that would reflect closed shells on all ions. It must be recognized, of course, that the Z^* values are dynamic only and reflect the effects of covalency with respect to some reference ionic value; however, the reference values here are unclear (except for Li, which clearly should be $+1$).

Due to the expected strong covalency in the B-C bonds, it perhaps is not surprising that the B and C effective charges are strongly altered from (smaller) reference ionic values. For $\hat{c}$-axis polarization, the Li value itself is unusual (almost 50% larger than its nominal value), indicating that Li is definitely involved in the interlayer coupling. We return to this important feature below. This partial Li covalency is probably connected with the difficulty in deintercalating it from the LiBC lattice.[6,7]

Another view of the charge response can be obtained from the "mode effective charges" defined by Gonze and Lee,[15] which for the symmetry of LiBC can be written for each polarization as

$$\vec{Z}^* = \sum_\kappa \frac{Z_\kappa^* \vec{U}_\kappa}{\sum_{\kappa'} \vec{U}_{\kappa'}^* \cdot \vec{U}_{\kappa'}}. \tag{1}$$

TABLE III. Mode effective charges of the IR-active optical modes.

Modes	Directions		
	a	b	c
Layer sliding E_{1u}	0.65	−1.37	0.00
	1.37	0.65	0.00
Layer beating A_{2u}	0.00	0.00	3.00
B-C puckering A_{2u}	0.00	0.00	−2.10
Bond stretching E_{2u}	−5.50	−0.10	0.00
	−0.10	5.50	0.00

Here each ion effective charge is weighted by the mode eigenvector that is normalized without the ion mass factor that occurs in the usual normalization of $U_{\kappa\alpha}$ (κ is the atom index, and α is the Cartesian coordinate). The mode effective charge vectors indicate how strongly a mode will couple to an electric field and are listed in Table III for the IR-active modes in LiBC. For the $\hat{c}$-axis-polarized modes, $|\vec{Z}^*|$ is 3.00 for the (softer) layer beating mode and 2.10 for the (harder) B-C puckering mode. For planar displacements, the (soft) layer sliding mode has the value 1.52 and the (hard) B-C bond stretching mode value is 5.50. These trends follow those found by Zhong *et al.* in perovskites,[17] where displacements that modulated the "covalent" bonding produced the largest mode effective charge. The value of 3.00 for the layer beating mode reflects the substantial Li "covalent" character for $\hat{c}$-axis displacements.

C. Infrared response

The static electronic dielectric constants are calculated to be $\epsilon_\infty^\perp = 12.95$, $\epsilon_\infty^\parallel = 11.24$. These values tend to be overestimated in local density approximation (LDA) calculations such as those used here, presumably due to the underestimation of the band gap. Dielectric constants are also somewhat dependent (at the ~5% level) on the choice of pseudopotential. According to the generalized Lyddane-Sachs-Teller (LST) relation

$$\epsilon_0 = \epsilon_\infty \prod_m \frac{\omega_{LO,m}^2}{\omega_{TO,m}^2}, \tag{2}$$

which is used separately for each polarization, the static dielectric constants ϵ_0 of both directions are 17.4 and 18.5, respectively. In the GHz range (~0.03 cm^{-1}), $\epsilon \approx 35$ was measured by Pronin *et al.*,[8] but this value is not necessarily expected to be intrinsic.

The relationship between the LO-TO splitting and the Born effective charges is given by the relation[15,18] (which holds for parallel and perpendicular vibrations separately)

$$\sum_m [\omega_{LO,m}^2 - \omega_{TO,m}^2] = \frac{4\pi}{\epsilon^\infty V_0} \sum_\kappa \frac{(Z_\kappa^* e)^2}{M_\kappa}$$

$$= \sum_\kappa \Omega_{ion,\kappa}^2 . \quad (3)$$

In this relation, m goes over the IR-active modes of the given polarization, M_κ the ionic mass of atom κ, V_0 the volume of the primitive unit cell, and the right-hand side has been expressed in terms of screened ionic plasma frequencies $\Omega_{ion,\kappa}$, which indicate how much each ion contributes to the combined strength of the resonances. For in-plane polarization, Li, B, and C contribute 6%, 26%, and 58%; the Li ion has minor effect and the response is dominated by B-C bond stretching. For $\hat{c}$-axis polarization, the contributions are 43%, 5%, and 51%, respectively; here the B is almost irrelevant, and the Li contribution is comparable to that of C.

The contributions can be examined mode by mode. The dielectric function can be expressed in terms of contributions from the IR-active modes (m) as

$$\frac{\epsilon(\omega)}{\epsilon^\infty} = 1 + \frac{4\pi}{\epsilon^\infty V_0} \sum_m \frac{S_m}{\omega_{TO,m}^2 - \omega^2}$$

$$= 1 + \sum_m \frac{\omega_{LO,m}^2 - \omega_{TO,m}^2}{\omega_{TO,m}^2 - \omega^2} . \quad (4)$$

The second line follows from the relation between the mode oscillator strength S_m and the corresponding LO-TO splitting, provided in Table I in terms of $\Delta\omega^2 = \omega_{LO}^2 - \omega_{TO}^2$. For in-layer polarization, large LO-TO splitting of the bond stretching E_{1u} mode at 1143 (1235) cm^{-1} is the result of the large B and C effective charges; the splitting of the layer sliding mode at 346 (371) cm^{-1} is an order of magnitude less. For c-axis polarization, the effective charges are ''derived'' 70% from the 407 (507) cm^{-1} layer beating mode with large LO-TO splitting involving the larger Z^* for Li, and only 30% derives from the 803 (828) cm^{-1} B-C puckering mode.

From Eq. (4) the zero-frequency limit is given by

$$\frac{\epsilon(\omega)}{\epsilon^\infty} - 1 = \sum_m \left(\frac{\omega_{LO,m}^2}{\omega_{TO,m}^2} - 1 \right), \quad (5)$$

which is different from the approximate ''generalized Lyddane-Sachs-Teller'' relation of Eq. (2), which is often quoted. It is not as different as it looks. The ''textbook'' form of the dielectric function in terms of its zeros and poles is

$$\frac{\epsilon(\omega)}{\epsilon^\infty} = \prod_m \frac{\omega_{LO,m}^2 - \omega^2}{\omega_{TO,m}^2 - \omega^2} . \quad (6)$$

While this expression has the same poles (at $\omega_{TO,m}$) as Eq. (4), the positions of its zeros, at $\omega_{LO,m}$ in this expression, are different from the zeros in the general expression Eq. (4). However, zeros have to occur between each of the poles, and the zeros of Eq. (4) are determined not only by $\omega_{LO,m}$ but also by the polarization arising from other LO modes with $m' \neq m$. The differences are small, however. For in-plane polarization, the zeroes of $\epsilon(\omega)$ from Eq. (4) are 367 cm^{-1} and 1236 cm^{-1} compared to the calculated ''LO'' frequencies of 371 and 1235 cm^{-1}, respectively. (Note that the lower is pushed down, while the higher is increased, for the case of two LO modes as we have here.) For $\hat{c}$-axis polarization, Eq. (4) gives 499 and 833 cm^{-1} compared to the calculated values of 507 and 828 cm^{-1}.

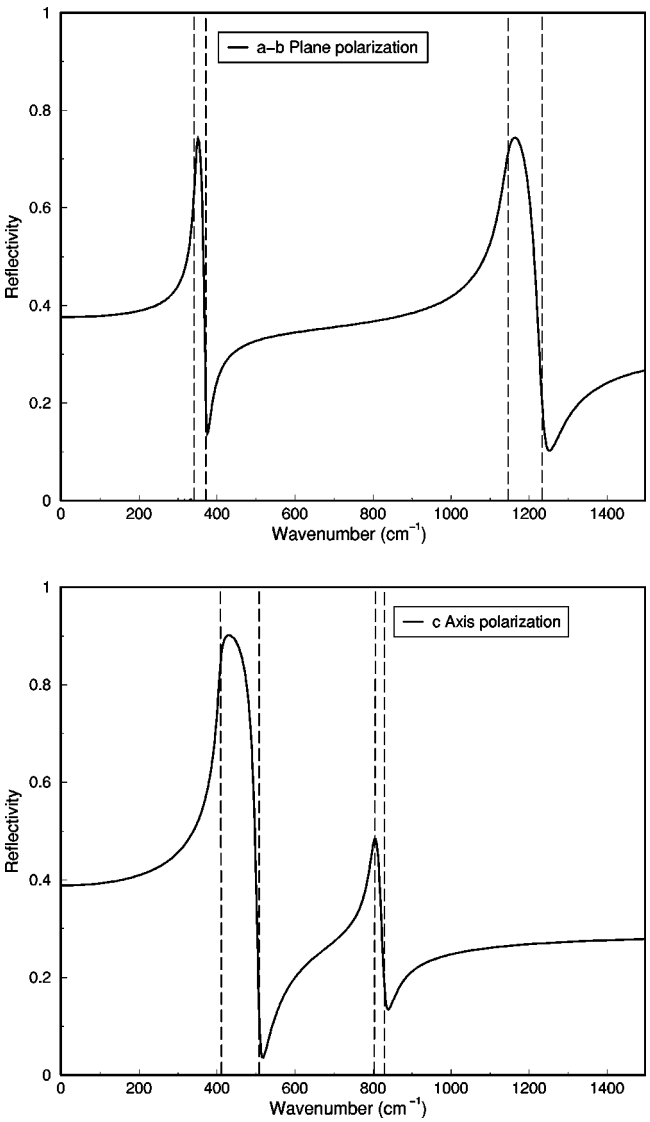

FIG. 2. Calculated reflectivity spectrum $R(\omega)$ for LiBC for polarization in the $a-b$ layer (top panel) and along the $\hat{c}$ axis (bottom panel), calculated from Eq. (6). The dashed lines mark the positions of the TO and LO modes for each IR-active mode (two of them for each polarization). The damping was chosen to be 3% of the frequency for each mode.

IV. DISCUSSION AND SUMMARY

The calculated Raman-active frequencies are in excellent agreement with the data of two groups.[5,6] The IR modes remain to be verified and understood. The spectra are polar-

ization dependent, and the spectra presented by Pronin *et al.*[8] and by Bharathi *et al.*[4] are not representative of pure polarization data.

Since it will be useful for comparison with single-crystal data, in Fig. 2 we present our predicted reflectivity $R(\omega)$ spectrum for both in-plane and perpendicular polarizations. The damping (which for a clean undoped sample would be due to anharmonicity) has been chosen for each mode to be 3% of the frequency (zero damping curves are not very representative). If the damping is not too large and there is no reason to expect large anharmonicity in LiBC, then both TO and LO frequencies can be obtained with small uncertainty.

It was mentioned in the Introduction that calculations have indicated that, if partial Li removal can be achieved, $Li_{1-x}BC$ should be a very good superconductor. Such Li extraction is common in many materials, being the process that forms the basis for Li batteries. What our studies here have shown is that (primarily for $\hat{c}$-axis displacements) Li shows considerable covalency with the B-C layer, with Li-C coupling being the prominent feature. This partial Li covalency is probably connected with the difficulty that several groups have found[6,7] in deintercalating it from the LiBC lattice. In addition, Cava, Zandbergen, and Inumaru noted briefly that LiBC seems to be highly resistant to chemical doping.[19]

The finding here that C is very different chemically from B in this system also carries some implications for C replacement of B in MgB_2. Recent studies confirm that about 10% of B can be replaced with C while retaining the structure, and the superconducting transition temperature remains high ($T_c = 22$ K).[20–22] If C alloying in the B sublattice were rigid band like, the additional 0.1 electron per cell would roughly half fill the important σ bands[23] that are responsible for superconductivity, and T_c would be expected to vanish (or nearly so). The great difference between C and B behavior in LiBC reflects strong differences in bonding and suggests something very different from rigid-band ''doping.'' Preliminary calculations for $MgB_{2-x}C_x$ (ordered supercells and virtual crystal) (Ref. 24) indeed indicate substantial non-rigid-band behavior: C is really different from ''B with an extra electron.''

Although calculations such as those described here have been found in several systems to be accurate, it is highly desirable to obtain polarized single-crystal IR data to confirm our predictions.

ACKNOWLEDGMENTS

W.E.P. acknowledges informative communicaitons with A. Loidl, K. Liu, and J. Hlinka. We have benefited greatly from the ABINIT project and from personal communication with X. Gonze. This work was supported by NSF Grant No. DMR-0114818.

[1] J. Nagamitsu *et al.*, Nature (London) **410**, 63 (2001).
[2] H. Rosner, A. Kitaigorodsky, and W. E. Pickett, Phys. Rev. Lett. **88**, 127001 (2002).
[3] M. Wörle, R. Nesper, G. Mair, M. Schwarz, and H. G. von Schnering, Z. Anorg. Allg. Chem. **621**, 1153 (1995).
[4] A. Bharathi, S. J. Balaselvi, M. Premila, T. N. Sairam, G. L. N. Reddy, C. S. Sundar, and Y. Hariharan, Solid State Commun. **124**, 423 (2002).
[5] J. Hlinka, I. Gregora, J. Pokorny, A. V. Pronin, and A. Loidl, Phys. Rev. B **67**, 020504 (2003).
[6] B. Renker, H. Schober, P. Adelmann, P. Schweiss, K.-P. Bohnen, and R. Heid, cond-mat/0302036 (unpublished).
[7] D. Souptel, Z. Hossain, G. Behr, W. Löser, and C. Geibel, Solid State Commun. **125**, 17 (2003).
[8] A. V. Pronin, K. Pucher, P. Lunkenheimer, A. Krimmel, and A. Loidl, Phys. Rev. B **67**, 132502 (2003).
[9] L. Zhao, P. Klavins, and K. Liu, J. Appl. Phys. **93**, 8653 (2003).
[10] J. M. An, H. Rosner, S. Y. Savrasov, and W. E. Pickett, Physica B **328**, 1 (2003).
[11] N. Troullier and J. L. Martins, Phys. Rev. B **43**, 1993 (1991).
[12] See URL http://www.abinit.org/ABINIT/Psps/LDA_TM/lda.html
[13] See the Appendix of S. Goedecker, M. Teter, and J. Hutter, Phys. Rev. B **54**, 1703 (1996).
[14] Z. H. Levine and D. C. Allan, Phys. Rev. Lett. **63**, 1719 (1989).
[15] X. Gonze and C. Lee, Phys. Rev. B **55**, 10 355 (1997).
[16] D. L. Rosseau, R. P. Bauman, and S. P. S. Porto, J. Raman Spectrosc. **10**, 253 (1981).
[17] W. Zhong, R. D. King-Smith, and D. Vanderbilt, Phys. Rev. Lett. **72**, 3618 (1994). Note that these authors used a somewhat different definition of the mode effective charge than was given by Gonze and Lee (Ref. 15).
[18] R. Resta, M. Posternak, and A. Baldereschi, Phys. Rev. Lett. **70**, 1010 (1993).
[19] R. J. Cava, H. W. Zandbergen, and K. Inumaru, Physica C **385**, 8 (2003).
[20] R. A. Ribeiro, S. L. Bud'ko, C. Petrovic, and P. C. Canfield, Physica C **385**, 16 (2003).
[21] T. Takenobu, T. Ito, D. H. Chi, K. Prassides, and Y. Iwasa, Phys. Rev. B **64**, 134513 (2001).
[22] M. Avdeev *et al.*, cond-mat/0301025 (unpublished).
[23] H. Rosner, J. M. An, W. E. Pickett, and S. L. Drechsler, Phys. Rev. B **66**, 024521 (2002).
[24] D. Kasinathan and W. E. Pickett (unpublished).